Table 1. Biological characterization of sPV1(M). Plaque reduction assay in the presence (+) and absence (−) of antibodies as described in (*13*). Anti-PV1(M) and anti-PV2(L) are neutralizing polyclonal antibodies specific for types 1 and 2 poliovirus, respectively. Neuropathogenicity of sPV1(M) and *wt* PV1(M) was assayed in hPVR-tg mice as described in (*13*). PLD_{50} is defined as the amount of virus that caused paralysis or death in 50% of the inoculated mice.

Virus	PFU						PLD_{50} (log$_{10}$ PFU)
	Mab D171		Anti-PV1(M)		Anti-PV2(L)		
	−	+	−	+	−	+	
sPV1(M)	83	0	91	0	88	92	6.2
wt PV1(M)	89	0	86	0	90	87	2.0

mice, resembling the disease produced by *wt* PV1(M) (*13*). However, a larger inoculum of sPV1(M) than PV1(M) was necessary to paralyze or kill the animals (Table 1). The increase in the magnitude of attenuation was unexpected, because all nucleotide substitutions introduced into sPV1(M) resulted in silent mutations in the ORF, except for the newly created Xma I and Stu I sites in the 5' nontranslated region (NTR) and 2B region, respectively. These latter changes had been shown previously to have no influence on viral replication in tissue culture (*20*, *21*). However, the silent mutations that we introduced into the poliovirus genome may exert a strong influence on pathogenesis by hitherto unknown mechanisms.

The presence or absence of genetic markers in the inoculated virus and the virus isolated from the spinal cords of paralyzed mice was confirmed by amplification of the viral RNA by RT-PCR and restriction enzyme analysis. Our results show that the viruses isolated from the spinal cords of paralyzed mice resembled the inoculated virus (fig. S1). Our data also confirm that the synthetic virus was the causative agent of the flaccid paralysis observed in the sPV1(M)-infected mice.

The chemical synthesis of the viral genome, combined with de novo cell-free synthesis, has yielded a synthetic virus with biochemical and pathogenic characteristics of poliovirus. In 1828, when Wöhler synthesized urea, the theory of vitalism was shattered (*22*). If the ability to replicate is an attribute of life, then poliovirus is a chemical

[$C_{332,652}H_{492,388}N_{98,245}O_{131,196}$- $P_{7501}S_{2340}$, see (*2*)] with a life cycle.

As a result of the World Health Organization's vaccination campaign to eradicate poliovirus (*23*), the global population is better protected against poliomyelitis than ever before. Any threat from bioterrorism will arise only if mass vaccination stops (*23*) and herd immunity against poliomyelitis is lost. There is no doubt that technical advances will permit the rapid synthesis of the poliovirus genome, given access to sophisticated resources. The potential for virus synthesis is an important additional factor for consideration in designing the closing strategies of the poliovirus eradication campaign.

References and Notes
1. F. L. Schaffer, C. E. Schwerdt, *Proc. Natl. Acad. Sci. U.S.A.* **41**, 1020 (1955).
2. A. Molla, A. Paul, E. Wimmer, *Science* **254**, 1647 (1991).
3. T. Pfister, C. Mirzayan, E. Wimmer, in *The Encyclopedia of Virology*, R. G. Webster, A. Granoff, Eds. (Academic Press Ltd., London, ed. 2, 1999), pp. 1330–1348.
4. N. Kitamura *et al.*, *Nature* **291**, 547 (1981).
5. V. R. Racaniello, D. Baltimore, *Proc. Natl. Acad. Sci. U.S.A.* **78**, 4887 (1981).
6. J. M. Hogle, M. Chow, D. J. Filman, *Science* **229**, 1358 (1985).
7. E. Wimmer, C. U. T. Hellen, X. Cao, *Annu. Rev. Genet.* **27**, 353 (1993).
8. C. L. Mendelsohn, E. Wimmer, V. R. Racaniello, *Cell* **56**, 855 (1989).
9. S. Koike *et al.*, *EMBO J.* **9**, 3217 (1990).
10. S. K. Jang *et al.*, *J. Virol.* **62**, 2636 (1988).
11. J. Pelletier, N. Sonenberg, *Nature* **334**, 320 (1988).
12. W. K. Xiang, A.V. Paul, E. Wimmer, *Semin. Virol.* **8**, 256 (1987).
13. Materials and methods are available as supporting material on *Science* Online.
14. S. van der Werf, J. Bradley, E. Wimmer, F. W. Studier, J. J. Dunn, *Proc. Natl. Acad. Sci. U.S.A.* **82**, 2330 (1986).
15. J. Cello, A. V. Paul, E. Wimmer, unpublished data.
16. P. Nobis *et al.*, *J. Gen. Virol.* **66**, 2563 (1985).
17. S. Koike *et al.*, *Proc. Natl. Acad. Sci. U.S.A.* **88**, 951 (1991).
18. H. Horie *et al.*, *J. Virol.* **68**, 681 (1994).
19. M. Gromeier, H.-H. Lu, E. Wimmer, *Microb. Pathog.* **18**, 253 (1995).
20. C. Mirzayan, E. Wimmer, *Virology* **189**, 547 (1992).
21. W. Xiang, K. S. Harris, L. Alexander, E. Wimmer, *J. Virol.* **69**, 3658 (1995).
22. F. Wöhler, *Ann. Phys. Chem.* **88**, 253 (1828).
23. A. Nomoto, I. Arita, *Nature Immunol.* **3**, 205 (2002).
24. We thank A. Wimmer and J. Benach for valuable comments on the manuscript. We are indebted to B. L. Semler for a sample of cell-free HeLa cell extract. Supported by Contracts N65236-99-C-5835 and N65236-00-M-3707 from the Defense Advanced Research Project Agency.

MAP Kinase Phosphatase As a Locus of Flexibility in a Mitogen-Activated Protein Kinase Signaling Network

Upinder S. Bhalla,[1]*† Prahlad T. Ram,[2]*† Ravi Iyengar[2]

Intracellular signaling networks receive and process information to control cellular machines. The mitogen-activated protein kinase (MAPK) 1,2/protein kinase C (PKC) system is one such network that regulates many cellular machines, including the cell cycle machinery and autocrine/paracrine factor synthesizing machinery. We used a combination of computational analysis and experiments in mouse NIH-3T3 fibroblasts to understand the design principles of this controller network. We find that the growth factor–stimulated signaling network containing MAPK 1, 2/PKC can operate with one (monostable) or two (bistable) stable states. At low concentrations of MAPK phosphatase, the system exhibits bistable behavior, such that brief stimulus results in sustained MAPK activation. The MAPK-induced increase in the amounts of MAPK phosphatase eliminates the prolonged response capability and moves the network to a monostable state, in which it behaves as a proportional response system responding acutely to stimulus. Thus, the MAPK 1, 2/PKC controller network is flexibly designed, and MAPK phosphatase may be critical for this flexible response.

Intracellular signaling pathways communicate extracellular information to modulate cellular functions in response to external stimuli. Signaling pathways function not only to transmit information but also to process the information as it is being transmitted. Such processing occurs because signaling pathways interact with one another to form networks (*1–3*). The processing occurs both through summation of inputs and through the temporal characteristics of pathways. For instance, the MAPK cascade communicates signals from growth factors that bind to receptor tyrosine kinases to the transcriptional

machinery and other cellular effectors (*4*, *5*). However, receptor tyrosine kinases activate other effectors such as phospholipase C–γ (PLC-γ), which leads to the activation of PKC (*6*). PKC in turn stimulates MAPK 1, 2 through activation of the protein kinase c-Raf (*7*). MAPKs activate cytoplasmic phospholipase-A2 (cPLA$_2$) (*8*, *9*). The arachidonic acid produced by cPLA$_2$ also stimulates PKC (*10*, *11*). These pairwise connections create a potential positive-feedback loop in the MAPK network (Fig. 1A). Such a simple network can function as a bistable switch wherein a brief extracellular stimulus results in sustained MAPK activation (*12*).

Signal flow through this MAPK network reflects a balance between the positive phosphorylation and the reverse dephosphorylation reactions. We therefore considered two key phosphatases in this system: protein phosphatase 2A (PP2A), a broad-specificity Ser-Thr phosphatase that dephosphorylates both Raf and MAP/ERK kinase (MEK) (*13*, *14*); and MAPK phosphatase (MKP), a dual-specificity phosphatase that dephosphorylates both Tyr and Thr residues on MAPKs and whose expression is transcriptionally regulated by MAPK (*15*). MAPK also phosphorylates MKP, which reduces ubiquitination and degradation of MKP (*16*). The increase in amounts of MKP constitutes a negative feedback. Computational analysis shows that MKP activity at specified levels and duration can limit the activated steady state of MAPK (*12*). Coupling the positive- and negative-feedback loop within the system could lead to oscillations. However, we had found although the system could move between regimes where it could exist at two (basal and activated) stable states (bistable) and one (basal) stable state, the system was not oscillatory (*17*). What then might be the systems function of MKP induction? Computational analysis suggests that at higher amounts of MKP, the network would function as a proportional-response system yielding differing amounts of activated MAPK for varying concentrations of growth factors, whereas at lower concentrations of MKP the system might function as an all-or-none switch at steady state. This hypothesis would suggest that the MAPK network is designed with the capability of mounting several types of responses, i.e., in a flexible manner. Indeed, one important question in biological systems is whether regulatory networks are flexibly designed.

We integrated computational analysis with experiments in NIH-3T3 fibroblasts to determine whether the MAPK controller network is flexibly designed.

We modeled the MAPK network with a system of coupled ordinary differential equations in the general neural simulator GENESIS with the Kinetikit interface (*18*). The detailed equations and constants have been described (*12*, *17*) and are provided in the supporting text (*19*). Initial simulations showed that after a brief (5 min) stimulation by a growth factor, MAPK activity remained elevated for an extended (30 to 45 min) period (Fig. 1B). As a result of system complexity related to MAPK-induced increases in the amounts of its negative regulator MKP, the activated state is temporally constrained, i.e., not maintained indefinitely. There was minimal decrease in the MAPK 1, 2 activity for up to 40 min, followed by a steady decline (Fig. 1B). We have operationally defined the activated steady state as a period that is at least five times longer than the initial stimulation (at least 25 min of high activity for 5-min stimulation by growth factor).

Under this temporal constraint, we computed the dependence of activation of cPLA$_2$ on MAPK and vice versa at steady state (25 to 40 min) after 5 min of stimulation (Fig. 1C). The system exhibits bistable behavior as seen by the three intersection points between the two computed concentration-effect curves (Fig. 1C). Initial stimulation by PDGF that raised MAPK or cPLA$_2$ activity above the levels defined by the middle metastable intersection point (denoted by number 2 in Fig. 1C) allows the system to come to an activated steady state (uppermost intersection point, number 3 in Fig. 1C) whereas the low-level stimulation results in the system relaxing to the basal state (lowermost intersection point, number 1 in Fig. 1C) as soon as the stimulus was withdrawn. We examined whether we could observe a similar profile experimentally (*19*). NIH-3T3 cells deprived of serum were stimulated with PDGF for 5 min. The cells were washed and the activation state of MAPK was determined by immunoblotting
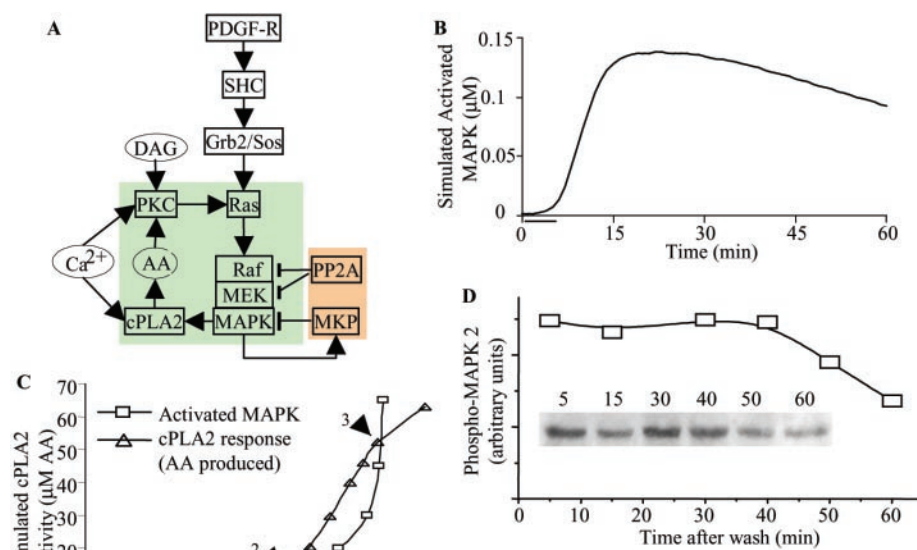

Fig. 1. The receptor tyrosine kinase, MAP kinase, and protein kinase C signaling network and feedback loop. (**A**) Block diagram of network. The components highlighted in green form the positive-feedback loop. The pathways highlighted in orange are inhibitory. This block diagram abstracts a complex network that is described in detail in the supplementary materials. Abbreviations: PDGFR, platelet-derived growth factor receptor; PKC, protein kinase C; AA, arachidonic acid; PP2A, protein phosphatase 2A; MEK, MAPK or ERK kinase; MAPK, mitogen-activated protein kinase 1, 2; cPLA$_2$, cytoplasmic phospholipase A$_2$; MKP, MAP kinase phosphatase; DAG, diacylglycerol. (**B**) Simulation of the levels of active MAPK at various time points after activation with 50 ng/ml PDGF for 5 min; the stimulus period is indicated by the bar at the bottom of the graph. (**C**) Intersecting concentration-effect curves for steady-state MAPK activation by cPLA$_2$ (□), and cPLA$_2$ activation by MAPK (△), plotted on the same axes. cPLA$_2$ activity is measured in terms of concentrations of AA, its product. MKP activity in these simulations is fixed at the initial levels of 2.4 nM total MKP (MKP-1 + MKP-2). The three intersection points define stable points of the system. Point 1 is the basal level of activity, point 2 is a metastable point, and point 3 is the high stable state of activity. (**D**) Activation state of MAPK in NIH-3T3 cells after stimulation with PDGF. Serum-starved cells were stimulated with 50 ng/ml PDGF for 5 min and then washed with serum-free medium. The cells were then reincubated in serum-free medium for various lengths of time. Protein from soluble cell lysate was probed with antibody specific for dual-phosphorylated MAPK (Phospho-MAPK 2).

[1]National Center for Biological Sciences, Bangalore 560065 India. [2]Department of Pharmacology and Biological Chemistry, Mount Sinai School of Medicine, New York, NY 10029, USA.

*These authors contributed equally to this work.
†Queries regarding computational analysis should be addressed to U.S.B. (e-mail: bhalla@ncbs.res.in) and experimental work to P.T.R. (e-mail: prahlad.ram@mssm.edu)

with antibody to the phosphophorylated forms of MAPK 1 and 2. MAPK activity increased within 5 min and stayed active for more than 40 min after removal of PDGF (Fig. 1D). Thus, for approximately eightfold duration of the initial stimulus the system stays stably active. Because the parameters used for the modeling are largely derived from in vitro measurements, often with purified proteins, there is no quantitative congruence between the simulations and the experiments conducted in the intact cell. However, the qualitative features predicted by the simulation were observable experimentally in an intact cell system.

If the persistently increased MAPK activity is due to the presence of a feedback loop, then inhibition of cPLA$_2$, a target of MAPK, should block the persistent activation of MAPK while allowing acute stimulation. Computational analysis indicated that this is indeed the case (Fig. 2A). Experimentally, NIH-3T3 cells were treated without or with arachidonyltrifluoromethyl ketone (AA-COF3), a selective inhibitor of cPLA$_2$ (*19*), then stimulated with a 5-min pulse of PDGF, washed, and assayed for activation of MAPK 1, 2. Treatment with the cPLA$_2$ inhibitor did not inhibit acute stimulation, but MAPK 1, 2 was not persistently activated (Fig. 2B). These results indicate that PKC may have a pivotal role in maintaining the feedback, because the arachidonic acid produced by cPLA$_2$ in conjunction with basal concentrations of diacylglycerol results in the stimulation of PKC at low Ca^{2+} (*20*). Hence, inhibition of PKC should block the persistent activation of MAPK 1, 2 and did so in computational experiments (Fig. 2C). In experiments, we used bisindolylmaleimide 1 (BIM1), an inhibitor of the typical forms of PKC, to determine if it blocked the persistent activation of MAPK. BIM1 does not affect the initial activation of MAPK 1, 2, but the activated MAPK 1, 2 returns to basal state within 30 min (*19*). Similar results were obtained when the levels of PKC were decreased by pretreatment with phorbol esters (*19*) (fig. S1). Thus, we observed a network of MAPK 1, 2, cPLA$_2$, and PKC in NIH-3T3 cells that behaves as a bistable system, i.e., moves between two stable states in a stimulus-dependent manner.

We next analyzed the role of MKP or any other protein phosphatase in regulating this bistable behavior. Because dephosphorylation of Raf and MEK by PP2A can also regulate bistability, we determined the ability of the network to exhibit bistable behavior at fixed varying concentrations of PP2A and MKP. At each paired concentration of phosphatases, we used concentration-effect analysis at steady state to obtain stable and metastable points (Figs. 1C and 3C). We obtained 2200 such concentration-effect curves. If a

single stable point was obtained, then the system existed in a monostable state. If two stable points and one metastable point were obtained, the system was in a bistable state. Figure 3A displays the results of these simulations in a perspective view in three dimensions. The breaking-wave–like bistable region in the center represents the bistable region. The same data viewed from above in two dimensions are shown in Fig. 3B. The bistable behavior denoted by diamonds occupies a defined region of parameter space, i.e., at paired ratios of PP2A to MKP. From the simulation in Fig. 3B, it can be seen that increasing concentrations of MKP at fixed concentrations of PP2A decreases the bistable region and would move the system into a monostable regime. To ascertain that at elevated MKP levels the system exhibited monostable behavior, we analyzed the effect of varying concentrations of active MAPK on activated cPLA$_2$ and vice versa. This computation is identical to that shown in Fig. 1C except for the higher MKP concentration (12 nM). There is a single intersection point at the

basal state of MAPK and cPLA$_2$ when MKP levels are increased by about fivefold (Fig. 3C). Because PP2A levels are very tightly controlled within the cell (*21*), we focused on MKP, which is induced by MAPK activation. Thus, with everything else in the system staying the same, the elevation of MKP levels would move the system into a monostable regime.

We tested the temporal effect of increasing MKP (concentrations and hence activity) on sustained MAPK activity (Fig. 3D). Here, a 5-min stimulatory pulse (e.g., PDGF stimulation) was applied and MAPK 1, 2 activity was followed for 90 min with different rates of MKP synthesis, thereby resulting in different amounts of steady-state MKP. At low concentrations of MKP, persistent activation is obtained, but at higher concentrations of MKP, upon withdrawal of the stimulus, the activated MAPK 1, 2 returns to the basal state. To provide an experimental frame of reference, we measured the amounts of MKP induced by MAPK activation. Treatment with PDGF results in a rapid increase in MKP
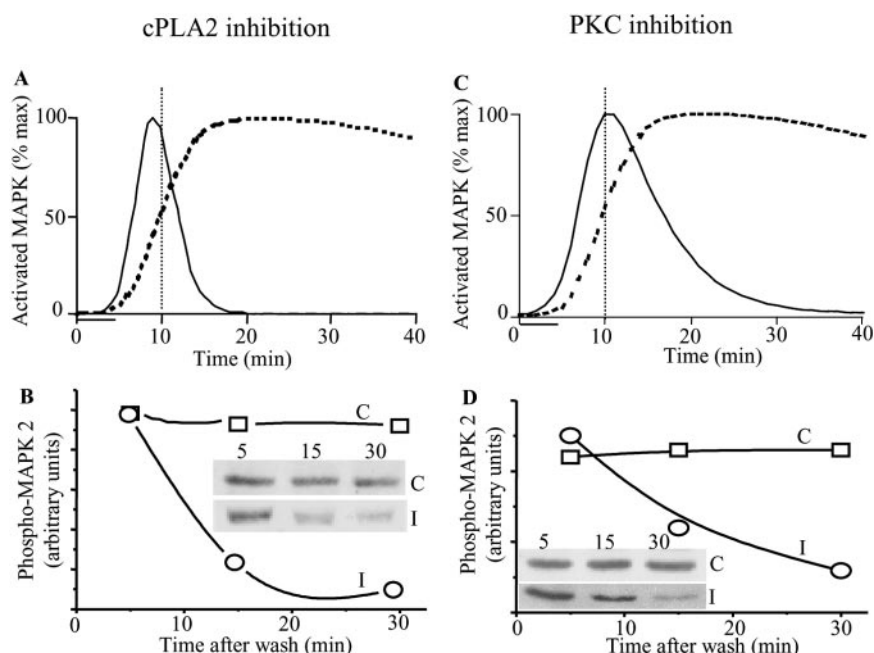

Fig. 2. Role of cPLA$_2$ and PKC activity in sustained MAPK activation. (**A**) Simulated values of MAPK activity at various time points after stimulation with 50 ng/ml PDGF for 5 min, with (dashed line) or without (solid line) cPLA$_2$ activity. The bar indicates the duration of stimulus, and the vertical dashed line corresponds to the first experimental time point as shown in (B). Simulated traces were independently scaled. (**B**) Effects of the cPLA$_2$ inhibitor on MAPK activity in NIH-3T3 cells after stimulation with PDGF and with (○) or without (□) the cPLA$_2$ inhibitor. Serum-starved cells were incubated with 10 μM AACOF$_3$ for 2 hours before stimulation with PDGF (50 ng/ml) for 5 min. The cells were washed with serum-free medium and reincubated for the times indicated. Proteins from soluble cell lysate were probed with antibody specific for dual-phosphorylated MAPK (Phospho-MAPK 2). (**C**) Simulated values of MAPK activity at various time points after stimulation with 50 ng/ml PDGF for 5 min, with normal (dashed line) or 80% blocked (solid line) PKC activity. The bar indicates the stimulus, and the vertical dashed line corresponds to the first experimental time point as shown in (B). (**D**) MAPK activity in NIH-3T3 cells after stimulation with PDGF and with (○) or without (□) PKC inhibitor. Serum-starved cells were incubated with 10 μM BIM1 for 30 min before stimulation with PDGF (50 ng/ml) for 5 min. The cells were washed with serum-free medium and reincubated for the times indicated. Proteins from soluble cell lysate were probed with antibody specific for dual-phosphorylated MAPK (Phospho-MAPK 2).

protein by about 30 min, and MKP stays elevated for over 2 hours (Fig. 3E). In cells containing threefold elevated levels of MKP (*19*), a 5-minute stimulation with PDGF increases activated MAPK 1, 2 briefly; removal of the stimulus results in a return to basal state within 30 min (Fig. 3F). To ascertain that this lack of prolonged activation was due to elevated MKP, we determined that transfection with MKP1 produced a similar effect (*19*) (fig. S2). Thus, it appears that elevation of MKP can push the MAPK 1, 2 system into a monostable regime in NIH-3T3 fibroblasts.
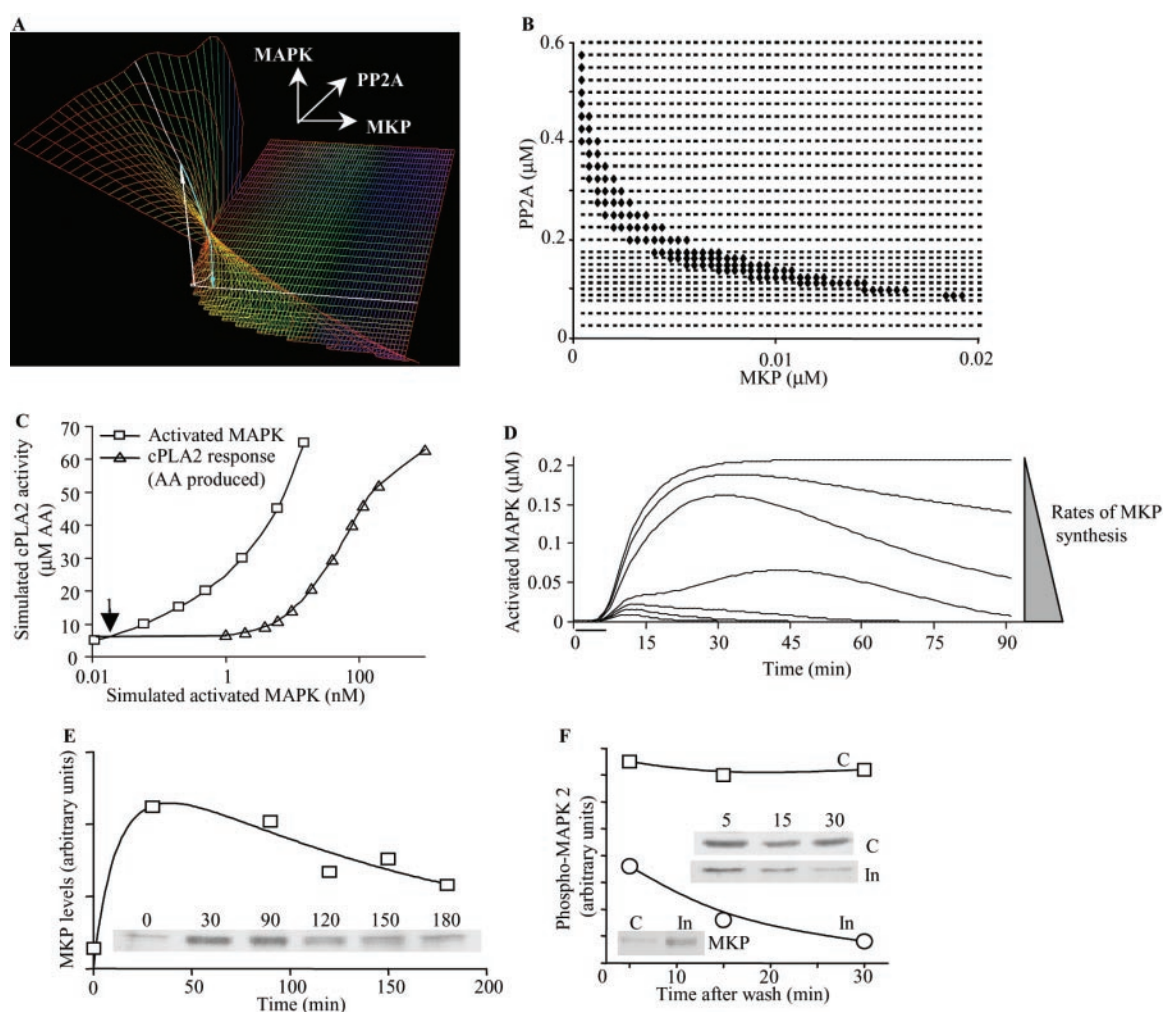
We next analyzed how the bistable and monostable MAPK 1, 2 system would respond to varying concentrations of PDGF. Computational analysis showed that when the system was capable of bistable behavior, a sharp threshold was observed when the effect of varying concentrations of PDGF on sustained activation of MAPK was measured (Fig. 4A). We determined if this could be observed in NIH-3T3 cells. We treated cells with varying concentrations of PDGF for 5 min. Cells were washed and incubated for 30 min and the activation state of MAPK 1, 2 was measured. A sharp transition between 5 and 10 ng/ml PDGF was observed (Fig. 4B). Thus, the bistable response works in a switchlike manner. When the amount of MKP is increased, the sustained switching response does not occur and the computational analysis shows an acute MAPK 1, 2 response that is proportional over at least a 10-fold concentration range of added growth factor (Fig. 4C). Thus, at high MKP concentrations the system behaves as a proportional-response system. To investigate whether this could be observed in the NIH-3T3 cells, we stimulated NIH-3T3 cells with PDGF for 5 min to increase MKP concentrations. The cells were washed, incubated for 60 min, and restimulated with varying concentrations of PDGF for 5 min, and the

Fig. 3. Role of MAPK phosphatase in regulating the bistable behavior. (**A**) Three-dimensional plot of the bistable behavior of MAPK/cPLA$_2$/PKC network as a function of regulation by PP2A and MKP. MKP feedback activation is disabled, and only steady-state MKP is applied at the plotted levels. The vertical axis measures feedback loop activity as MAPK activity. The upper region represents a state of high activity, and the lower plane one of low activity. In the intermediate "breaking wave" region, the curves fold around from the upper to the lower state, and thus this comprises a bistable region where both states can exist. The white curve represents the system response at varying levels of MKP at the reference level of 0.225 μM PP2A. The white arrow indicates the trajectory of system upon PDGF stimulation and elevation to a state of high activity. The cyan arrow indicates the trajectory as MKP-1 builds up, and eventually turns off the feedback-loop activity. (**B**) Regions of monostable (dashes) and bistable (diamonds) behavior of the feedback system. This is equivalent to looking at plot B from above. There is a large range of combinations of PP2A and MKP activities over which bistability will occur. (**C**) Concentration-effect curves for steady-state MAPK activation by PLA$_2$ (○), and PLA$_2$ activation by MAPK (△), plotted on the same axes. cPLA$_2$ activity is measured in terms of concentrations of AA, its product. MKP activity in these simulations is fixed at the induced levels of 12 nM total MKP (about five times basal level). The intersection point (arrow) defines the one low-activity stable point of the system. (**D**) Sustained MAPK activity is dependent on the rates of MKP synthesis and the resultant steady-state MKP levels. In this simulation a 5-min activation with PDGF is followed with varying rates of MKP synthesis. MAPK activity is plotted as a function of time as MKP is being synthesized. (**E**) MKP levels following PDGF stimulus in NIH-3T3 cells. Serum-starved cells were stimulated with PDGF (50 ng/ml) for 5 min, washed, and reincubated in serum-free medium for the times indicated. Proteins from soluble cell lysate were probed with antibody for MKP. (**F**) Effect of MKP levels on sustained activation of MAPK. Serum-starved NIH-3T3 cells were stimulated with PDGF (50 ng/ml) for 5 min (○) or vehicle (□), washed, and reincubated for 60 mins in serum-free medium. The cells were restimulated with PDGF (50 ng/ml) for 5 min, washed, and reincubated in serum-free medium for the times indicated. Proteins from soluble cell lysate were probed with antibody specific for dual-phosphorylated MAPK (Phospho-MAPK2). (Inset) Lysate probed for MKP, showing that levels of MKP are higher in the cells after the prepulse of PDGF followed by incubation for 60 min.

activity state of MAPK was determined. Increasing concentrations of PDGF gave correspondingly increasing amounts of MAPK 1, 2 activity from 0.5 to 10 ng/ml of PDGF (Fig. 4D). Thus, at elevated concentrations of MKP, the MAPK network is monostable and behaves only as a proportional-response system. MKP does not appear to have a role in the acute deactivation of MAPK (22) (Figs. 2 and 3). Knockout of MKP1 also does not yield an acute phenotype (23). The acute deactivation is likely to be controlled by PP2A dephosphorylating Raf and MEK and by other phosphatases working at the level of MAPK 1, 2. Thus, the role of the increased MKP expression appears to be to determine the system response capabilities to subsequent stimuli as shown below.

One of the functions of signaling networks is to confer adaptability to cellular responses. We examined whether a previous stimulus-and-response history could influence subsequent responses of the system to a new stimulus. To analyze this computationally, we stimulated the network with varying concentrations of PDGF for 5 min; the stimulus was then removed, and after 60 min, a saturating stimulus of 50 ng/ml PDGF was delivered for 5 min followed by removal of the stimulus. MAPK activity was followed as a function of time (Fig. 5A). This dual stimulus protocol illustrates the effects of prior history of stimulation on later responses to stimuli. Computationally, we found that the final sustained MAPK activity depends on the concentration of the PDGF prepulse. Only concentrations of PDGF that were initially below the threshold elicited a switchlike response to the second stimulus (Fig. 5B). The observed response shows a sharp threshold with the same half-maximum as for turn-on of the MAPK bistable state, but with the opposite slope. We experimentally measured MAPK activity at the final time point, 30 min after the second stimulus (Fig. 5C) (19). Cells that were initially stimulated with concentrations of PDGF that are above the threshold, to elicit a prolonged MAPK response and therefore an increase in MKP, are no longer able to sustain a prolonged MAPK response upon restimulation with a suprathreshold stimulus. Thus, it appears that the network adapts to a stimulus such that if the stimulus is greater than the threshold and elicits a switchlike response, a subsequent suprathreshold stimulus does not elicit a second switchlike response. Conversely, if the initial stimulus is below threshold and does not elicit a sustained response, a subsequent suprathreshold stimulus is now capable of eliciting a switchlike response. This flexibility of the networ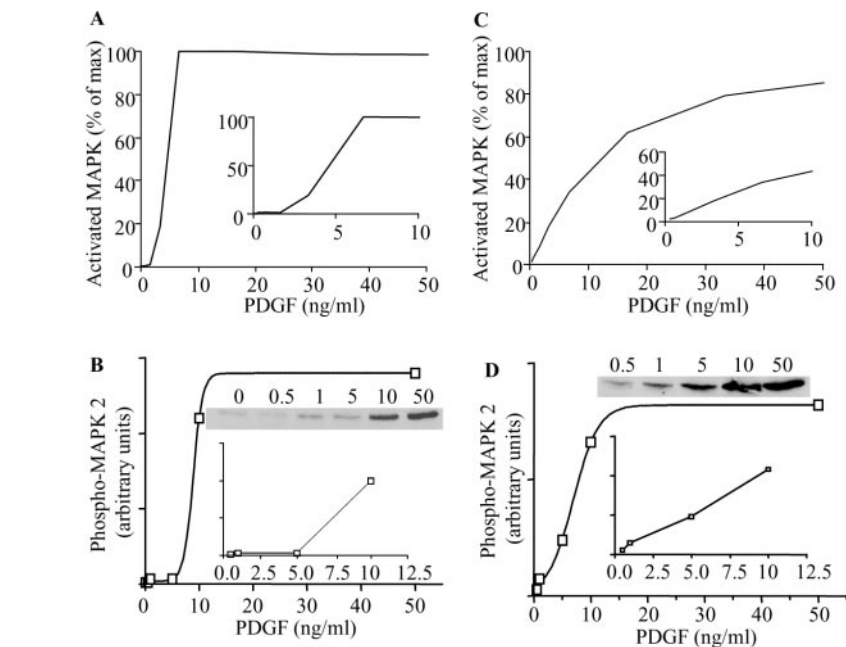k confers upon it the ability to respond to a series of stimuli in different ways depending upon the prior history of stimulus.

Our integrated computational and experimental analyses show that the MAPK system in some mammalian cells is flexibly designed such that it can move between bistable and monostable regimes in a self-regulated manner because activation of MAPK increases the amounts of MKP both by de novo synthesis and by direct phosphorylation to block degradation. Such self-regulated flexibility is likely to be an important characteristic of biological devices, necessary for biological systems to adapt and survive. The MAPK 1, 2 pathway is capable of regulating multiple cellular machines, including the transcriptional machinery, to stimulate the expression of cyclins that trigger entry into the cell cycle and the synthesis of arachidonic acid, a precursor for many autocrine and paracrine factors. It would not be advantageous to the cell if, every time an autocrine or paracrine factor needed to be synthesized, the cell were pushed into the cell cycle. Because sustained MAPK activity is required to reenter the cell cycle (24), it is possible that increased MKP concentrations allow the MAPK network to respond to external stimulation to control the biochemical machinery without engaging the cell-cycle machinery.

It is paradoxical that although the bistable behavior is a systems property as a whole, MKP appears to be the locus of flexibility. Thus, MKP can be thought to have distinct properties at two levels: At the molecular level, MKP is a dual-specificity phosphatase; at the systems level, MKP functions as the locus of flexibility that determines whether or not the system exhibits bistable behavior. This is the second phosphatase that we have found to play a determinant role in systems behavior. In the adenosine 3,5-monophosphate–α-calcium-calmodulin–dependent kinase II (cAMP-CAM-kinase II) network, protein phosphatase–1 gates signal flow through the CAM-kinase II pathway during the induction of long-term potentiation of synaptic responses (25). Perhaps other negative regulators of signaling such as phosphatases, phosphodiesterases, and GTPase-activating proteins also endow signal networks with unique systems capabilities.
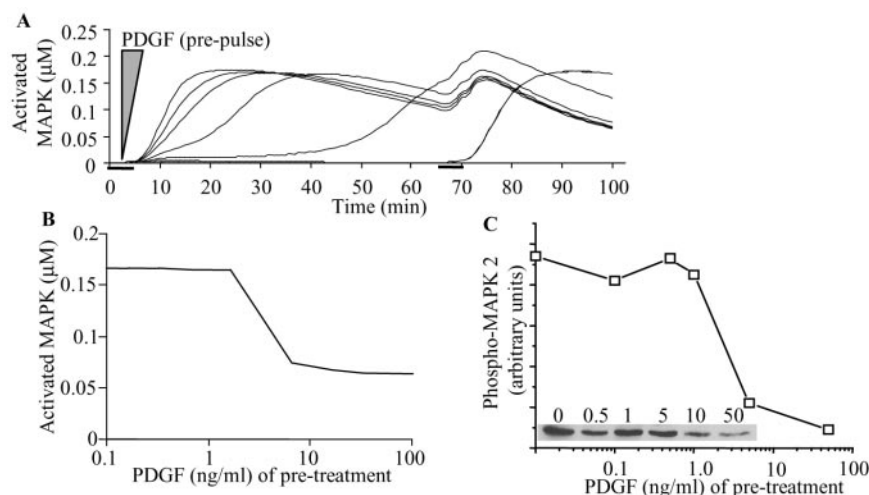

Fig. 4. Effects of varying concentrations of PDGF on MAPK activity at low and high MKP levels. (**A**) Simulation of MAPK response to varying concentrations of PDGF at basal MKP levels. (Inset) Enlargement of the same curve from 0 to 10 ng/ml. (**B**) PDGF concentration-effect curve in NIH-3T3 cells. Serum-starved NIH-3T3 cells were stimulated with various concentrations of PDGF for 5 min, washed, and reincubated for 30 min in serum-free medium. Proteins from soluble cell lysate were probed with antibody specific for dual-phosphorylated MAPK (Phospho-MAPK 2). (Inset) Enlargement of the curve from 0 to 10 ng/ml PDGF. The threshold is within experimental accuracy given the conversion 1 ng/ml = 30 pM PDGF. (**C**) Simulation of MAPK response to varying concentrations of PDGF at elevated MKP levels (0.01 μM, about four to five times basal). (**D**) Effects of varying concentrations of PDGF on MAPK activity in NIH-3T3 cells at high MKP levels. Serum-starved NIH-3T3 cells were stimulated with 50 ng/ml PDGF for 5 min, washed, and reincubated for 60 min in serum-free medium. The cells were then restimulated with various concentrations of PDGF for 5 min. Proteins from soluble cell lysate were probed with antibody specific for dual-phosphorylated MAPK (Phospho-MAPK 2). (Inset) Enlargement of the concentration-effect curve from 0 to 10 ng/ml PDGF.

Fig. 5. History-dependent responses of the MAPK system. A varying concentration of PDGF was delivered for 5 min, followed by a wash and reincubation. After 60 min a second stimulation was delivered at 50 ng/ml, which is normally saturating to elicit prolonged MAPK activation. (**A**) Computational traces show range of response time-courses. Initial and second stimulation durations are indicated by horizontal bars. Concentrations of PDGF during the initial stimulation are 20 pM (0.67 ng/ml), 100 pM (3.33 ng/ml), 200 pM (6.67 ng/ml), 500 pM (16.67 ng/ml), 1 nM (33.33 ng/ml), and 100 nM (333.33 ng/ml). (**B**) Computationally derived MAPK activities at the final time point, 100 min after start. (**C**) Effects of pretreatment of NIH-3T3 cells with varying concentrations of PDGF on subsequent stimulation by a saturating concentration. Serum-starved NIH-3T3 cells were stimulated with various concentrations of PDGF as indicated for 5 min, washed, and reincubated for 60 min in serum-free medium. The cells were then restimulated with 50 ng/ml PDGF for 5 min, washed, and incubated for 30 min. Proteins from soluble cell lysate were probed with antibody specific for dual-phosphorylated MAPK (Phospho-MAPK 2).

Current experimental techniques allow us to observe the predicted systems behavior only in a qualitative manner. To determine quantitative accuracy of our models, techniques that quantitatively and selectively measure biochemical reactions within the cell must be developed. Nevertheless, this first glimpse into the systems capabilities of a well-understood and widely used cell signaling system allows us to start unraveling the underlying complexity in nature's design of this controller network.

References and Notes
1. J. D. Jordan, E. M. Landau, R. Iyengar, *Cell* **103**, 193 (2000).
2. D. Bray, *Nature* **376**, 307 (1995).
3. G.Weng, U. S. Bhalla, R. Iyengar, *Science* **284**, 92 (1999).
4. T. J. Hemesath, E. R. Price, C. Takemoto, T. Badalian, D. E. Fisher, *Nature* **391**, 298 (1998).
5. R. J. Davis, *J. Biol. Chem.* **268**, 14553 (1993).
6. S. Nishibe *et al.*, *Science* **250**, 1253 (1990).
7. K. W. Wood, C. Sarnecki, T. M. Roberts, J. Blenis, *Cell* **68**, 1041 (1992).
8. L. L. Lin *et al.*, *Cell* **72**, 269 (1993).
9. R. A. Nemenoff *et al.*, *J. Biol. Chem.* **268**, 1960 (1993).
10. Y. Nishizuka, *Science* **258**, 607 (1992).
11. T. Shinomura, Y. Asaoka, M. Oka, K. Yoshida, Y. Nishizuka, *Proc. Natl. Acad. Sci. U.S.A.* **88**, 5149 (1991).
12. U. S. Bhalla, R. Iyengar, *Science* **283**, 381 (1999).
13. P. Dent, T. Jelinek, D. K. Morrison, M. J. Weber, T. W. Sturgill, *Science* **268**, 1902 (1995).
14. N. Gomez, P. Cohen, *Nature* **353**, 170 (1991).
15. H. Sun, C. H. Charles, L. F. Lau, N. K. Tonks, *Cell* **75**, 487 (1993).
16. J. M. Brondello, J. Pouyssegur, F. R. McKenzie, *Science* **286**, 2514 (1999).
17. U. S. Bhalla, R. Iyengar, *Chaos* **11**, 221 (2001).
18. U. S. Bhalla, in *The Book of GENESIS, Exploring Realistic Neural Models with GEneral NEural SImulation SYstem*, J. M. Bower, D. Beeman, Eds. (Springer-Verlag, Berlin, ed. 2, 1998), chap. 10.
19. Supplementary material is available on *Science* Online.
20. M. S. Shearman, Z. Naor, K. Sekiguchi, A. Kishimoto, Y. Nishizuka, *FEBS Lett.* **243**, 177 (1989).
21. Z. Baharians, A. H. Schonthal, *J. Biol. Chem.* **273**, 19019 (1998).
22. D. R. Alessi *et al.*, *Curr. Biol.* **5**, 283 (1995).
23. K. Dorfman *et al.*, *Oncogene* **13**, 925 (1996).
24. G. Pages *et al.*, *Proc. Natl. Acad. Sci. U.S.A.* **90**, 8319 (1993).
25. R. D. Blitzer *et al.*, *Science* **280**, 1940 (1998).
26. We thank R. Blitzer for critical reading of the manuscript. We also thank the anonymous reviewers for their incisive comments that were most useful in revising this paper. This research was supported by NIH grants GM-54508 and CA-81050 (R.I.) and the Wellcome Trust and NCBS funds (U.S.B.). P.T.R. was supported by an NIH postdoctoral fellowship (grant CA-79134).

Est1p As a Cell Cycle–Regulated Activator of Telomere-Bound Telomerase

Andrew K. P. Taggart, Shu-Chun Teng,* Virginia A. Zakian†

In *Saccharomyces cerevisiae*, the telomerase components Est2p, *TLC1* RNA, Est1p, and Est3p are thought to form a complex that acts late during chromosome replication (S phase) upon recruitment by Cdc13p, a telomeric DNA binding protein. Consistent with this model, we show that Est1p, Est2p, and Cdc13p are telomere-associated at this time. However, Est2p, but not Est1p, also binds telomeres before late S phase. The *cdc13-2* allele has been proposed to be defective in recruitment, yet Est1p and Est2p telomere association persists in *cdc13-2* cells. These findings suggest a model in which Est1p binds telomeres late in S phase and interacts with Cdc13p to convert inactive, telomere-bound Est2p to an active form.

In *S. cerevisiae*, telomeric DNA consists of irregular $C_{1-3}A/TG_{1-3}$ double stranded repeats as well as the G tail, a >30 nucleotide single-stranded overhang of TG_{1-3} DNA that is detectable only in late S phase (*1*, *2*). Telomere length is maintained by telomerase, a specialized reverse transcriptase with an integral RNA template. In yeast, telomerase action requires at least five genes, deficiencies in any or all of which lead to the same *est* (ever shortening telomeres) phenotype, a progressive telomere shortening leading to eventual cell death (*3*). *EST2* and *TLC1* encode the reverse transcriptase and RNA subunit, respectively. Telomerase action in vivo also requires Est1p, Est3p, and Cdc13p, a protein that binds single-stranded TG_{1-3} DNA. A current model for telomerase regulation is that Cdc13p binds G tails in late S phase to recruit a telomerase holoenzyme consisting of Est1p, Est2p, Est3p, and *TLC1* RNA (*4–*

Department of Molecular Biology, Princeton University, Princeton, NJ 08544, USA.

*Present address: Department of Microbiology, College of Medicine, National Taiwan University, Taiwan.
†To whom correspondence should be addressed. E-mail: vzakian@molbio.princeton.edu